Universal quenching of the superconducting state of two-dimensional nanosize Pb-island structures

Jungdae Kim, Gregory A. Fiete, Hyoungdo Nam, A. H. MacDonald, and Chih-Kang Shih*
Department of Physics, The University of Texas at Austin, Austin, Texas 78712, USA
(Received 24 October 2010; revised manuscript received 25 May 2011; published 27 July 2011)

We systematically address superconductivity of Pb nano-islands with different thicknesses and lateral sizes via a scanning tunneling microscopy/spectroscopy (STM/STS). Reduction of the superconducting gap (Δ) is observed even when the island is larger than the bulk coherence length (ξ) and becomes very fast below ~50-nm lateral size. The suppression of Δ with size depends to a good approximation only on the volume of the island and is independent of its shape. Theoretical analysis indicates that the universal quenching behavior is primarily manifested by the mean number of electronic orbitals within the pairing energy window.

DOI: 10.1103/PhysRevB.84.014517 PACS number(s): 74.78.−w, 73.21.Fg, 74.55.+v

The remarkable properties of a superconductor are attributable to its Cooper pair condensate (formed from a macroscopic number of electrons), which can be described by a single quantum wave function. According to the celebrated Bardeen-Cooper-Schrieffer (BCS) theory of superconductivity,[1] there is a minimum length scale (the coherence length ξ) on which the condensate-order parameter can vary. The fate of superconductivity in systems with spatial dimensions smaller than the coherence length ξ has been the subject of intense interest for decades because it is dependent on quantum confinement, interaction, and quantum-coherence effects in intrinsically many-particle context–ingredients that drive much modern research in quantum many-body physics.[2–21] Attention has often focused on two-dimensional (2-d) systems which can have fragile order because of quantum and thermal fluctuations. In this context the recent discovery of *robust* superconductivity in epitaxial thin Pb films with thicknesses that are orders of magnitude smaller than ξ seems surprising.[4,10,11] Even at a thickness of only two atomic layers (~0.6 nm), the superconducting transition temperature ($T_C \sim 5$ K) of Pb films is only slightly smaller than the bulk value 7.2 K.[4] Nevertheless, there remain disputes regarding the thickness dependence of T_C at thickness below 10 monolayers (MLs). Although this observation is already interesting, much more telling information on the fate of superconductivity at small length scales emerges when the lateral dimensions of the ultrathin films are also reduced.

What happens if all dimensions are reduced? Ultimately at some length scale, superconductivity should cease to exist. What determines this scale? Here we systematically address this fundamental question via a detailed scanning tunneling microscopy/spectroscopy (STM/STS) study of thin-film superconducting islands with different thicknesses and lateral sizes. By controlling the lateral size of ultrathin 2-d islands, we discovered that as the lateral dimension is reduced, suppression of the superconducting order occurs. The reduction of the superconducting order parameter starts slowly but then accelerates dramatically when the level spacing starts to approach the value of the gap. While the values of the superconducting gap of the nano-islands show thickness dependence at all lateral sizes, when normalized to the extended film limit they collapse to a universal curve that depends only on the volume of the nano-island. Most surprisingly, our results for the size of the gap Δ versus island volume show quantitative agreement with recent STS studies of hemisphere-shaped Pb droplets despite their dramatic difference in geometry.[5,9]

The experiments were conducted in a home-built low-temperature (LT) STM system with an *in situ* sample preparation chamber. The striped incommensurate (SIC) phase of the Pb-Si surface shown in Fig. 1(a) was prepared by deposition of ~1 ML of Pb onto the Si(111) 7×7 surface at room temperature, followed by sample annealing at 400 ~ 450 °C for 4 min to form the surface template.[22–24] Depending on the detailed kinetic control, either flat film or 2-d nano-islands of Pb can be obtained. Flat films can be grown by holding the sample temperature at ~100 K during Pb deposition.[4] Figure 1(b) shows a 5-ML film grown on the Pb-on-Si (111) SIC surface. In order to get 2-d islands with a variety of lateral sizes and thickness, Pb was deposited on the template at ~200 K with a deposition rate of 0.5 ML per minute. Figure 1(c) shows 2-d islands of different sizes and shapes on the same substrate. Also shown in Fig. 1(d) is a close-up view of two 3-ML 2-d islands, one with an effective diameter (d_{eff}) of 74 nm and one with an effective diameter of 15 nm. The effective diameter (d_{eff}) of each island is calculated by using $d_{\text{eff}} = \sqrt{ab}$, where a and b are lengths along the major and minor axes, respectively.

Figure 2(a) shows dI/dV tunneling spectra acquired at 4.3 K for a 5-ML film and 5-ML 2-d islands of various effective diameters. Interestingly even at a diameter of 235 nm, which is much larger than the bulk coherence length ξ (~80 nm), one already observes a small reduction of the superconducting gap in comparison to that of the extended film. As one can observe directly from the data, the trend toward gap reduction continues as the diameter of the 2-d islands decreases further. Figure 2(b) shows dI/dV tunneling spectra acquired at 4.3 K for 3-ML 2-d islands with diameters ranging from 15 nm to 74 nm. The size dependence of the superconducting gap of 4-ML 2-d islands follows a similar trend to that of 3-ML islands. It is important to recognize that as long as the individual island is isolated, the measured superconducting gap is very uniform throughout the island until its very edge.

Recently, Brun *et al.*[15] reported a study of thickness dependence of the superconducting gap of Pb 2-d islands with lateral size larger than ξ, which they interpreted to represent the superconducting properties of extended films. They found that the superconducting gap scales with the inverse of island thickness (1/d) and superconductivity should vanish at a

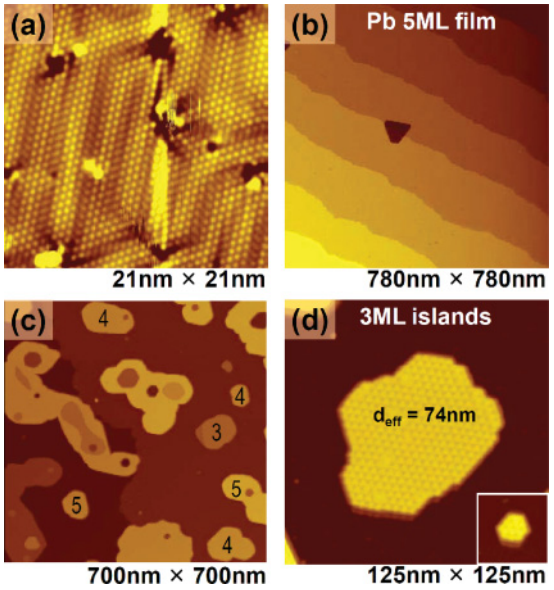

FIG. 1. (Color online) STM topography image of (a) the SIC phase of Pb-Si surface, (b) a globally uniform 5-ML Pb film, and (c) 2-d Pb islands with various lateral sizes and thicknesses. The numbers labeled on the image (c) indicate thickness of islands in ML. (d) Two 3-ML Pb islands with effective lateral size (d_{eff}) of 74 nm and 15 nm (inset) are shown in the same length scale (sample bias V_s = (a,d) 0.3 V, (b,c) 2 V, tunneling current I = (a) 20 pA, (b,c,d) 10 pA).

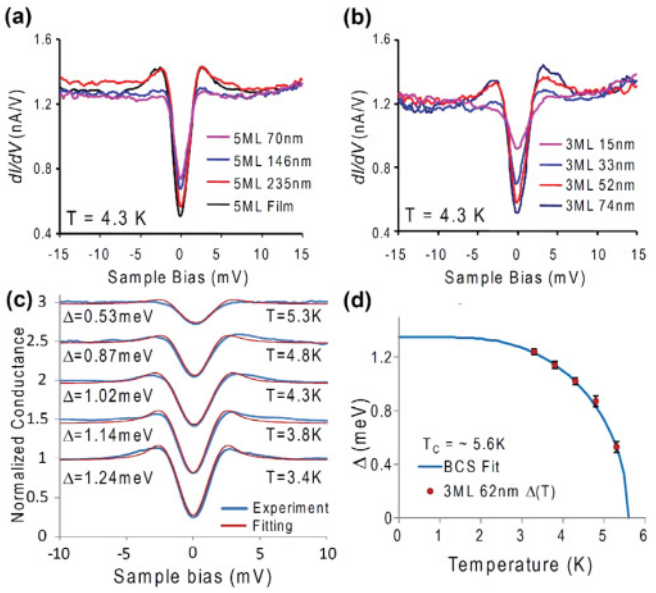

FIG. 2. (Color online) Lateral size dependence of differential conductance spectra (dI/dV) measured at 4.3 K is shown for (a) 5-ML islands and (b) 3-ML islands. All differential conductance spectra were taken with the same tunneling parameter with the junction stabilized at $V_s = 20$ mV and $I_t = 30$ pA tunneling current. (c) Normalized conductance spectra (blue) measured as a function of temperature from a 3-ML Pb island with a 62-nm-lateral size were fitted using the BCS DOS for the tunneling conductance (red). Each normalized spectrum is offset successively by 0.5 for clarity. (d) The superconducting energy gaps (Δ) for each temperature were obtained from (c) and plotted as red circles. The blue curve is a fitting of these energy gap data using a BCS gap equation to obtain a T_C of $\sim 5.6 \pm 0.1$ K for a 3-ML island with 62-nm-lateral size. All T_C values determined from such fitting are estimated to have an error bar of ± 0.1 K.

thickness of 2 ML. While the recent observation of strong superconductivity at 2 ML already implied the breakdown of the $1/d$ scaling,[4] the current result that gap reduction occurs in 2-d islands with lateral dimension much less than ξ should settle the true behavior of superconductivity in these nano-systems.

In order to more quantitatively characterize the suppression of superconductivity, we measured the transition temperature T_C for different lateral sizes and thicknesses of 2-d islands. To extract an energy-gap value for different temperatures $\Delta(T)$ we fit the normalized dI/dV spectrum measured by STS to BCS-like density of states (DOS), as shown in Fig. 2(c). All STM signals were carefully shielded against radio frequency (RF) noise, and a Gaussian-broadening parameter was implemented in the fitting to model the effect of the remaining noise. A standard deviation of 0.3 mV_{rms} was used for the Gaussian broadening (see Appendix A for more details). To determine T_C, extracted values of $\Delta(T)$ are fitted to the BCS-gap equation [see Fig. 2(d)];

$$\frac{1}{N(0)V} = \int_0^{E_D} \frac{1}{\sqrt{\varepsilon^2 + \Delta(T)^2}} \tanh\left(\frac{\sqrt{\varepsilon^2 + \Delta(T)^2}}{2k_B T}\right) d\varepsilon, \tag{1}$$

where $N(0)$ is the DOS at the Fermi level, V is the electron-phonon coupling, and E_D is the Debye energy. Strictly speaking the universal curve in Δ vs T is valid for a weak-coupling superconductor ($E_D/k_B T_C \gg 1$), but it is a good approximation in most cases, including Pb.[5,25]

Figure 3(a) demonstrates that T_C of 3-ML, 4-ML, and 5-ML islands depends on their lateral size d_{eff}. Interestingly there is a transition region (somewhere between 40 to 60 nm) below which electrons rapidly lose the strength of superconducting coherence. We also observe a variation of T_C as a function of island thickness for a given d_{eff}: T_C (3 ML) > T_C (4 ML) > T_C (5 ML), attributable to the quantum oscillations of T_C from the vertical electronic confinement, a topic that has been intensively investigated recently[4,19] (3-ML data was previously unavailable because of difficulty in preparing 3-ML films). The transition region from slow to rapid T_C reduction also shows thickness dependence: it occurs at $\sim$40 nm for 5-ML islands, at $\sim$50 nm for 4-ML islands, and slightly above 50 nm for 3-ML islands. On the other hand if we normalize the T_C of 2-d islands to the thin-film value at a given thickness and plot it as a function of island volume, the data collapse onto a single curve, revealing a universal behavior of superconductivity suppression with respect to the island volume [Fig. 3(b)]. Remarkably this universal curve is in quantitative agreement with earlier STS studies for Pb droplets, despite the dramatic difference in geometry.[5,9] This collapse demonstrates that superconductivity in regularly shaped nano-islands is sensitive to a large degree only to the average level spacing of a nano-structure, affirming to a surprisingly degree theories[7,8,26] of finite-size superconductivity suppression in which the mean number of electronic orbitals within the pairing energy window plays the central role.

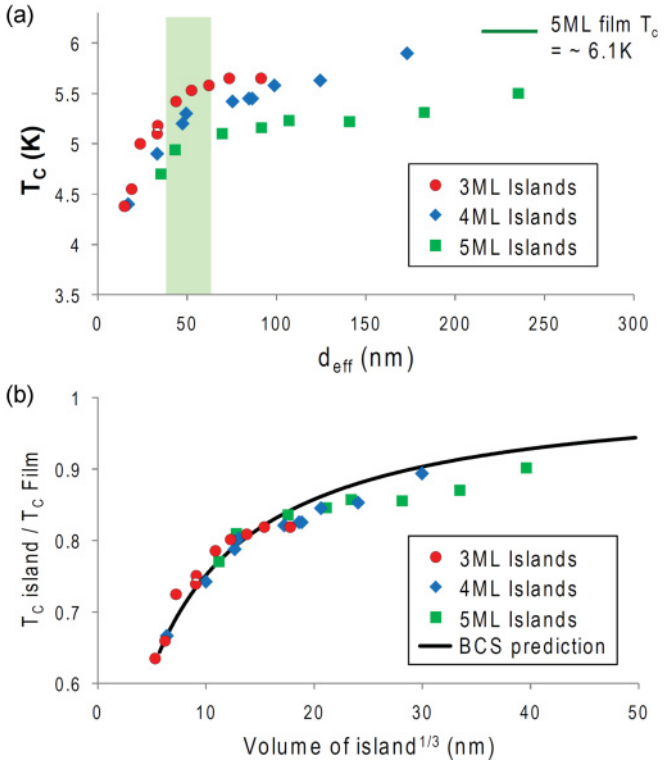

FIG. 3. (Color online) (a) T_C as a function of island lateral size for 3-ML, 4-ML, and 5-ML islands. A transition region from slow to dramatic reduction of superconductivity is shaded in green. (b) T_C of islands was normalized to the globally flat film T_C for each thickness and plotted as a function of cube root of island volume. For the T_C normalization, 5-ML film T_C was measured to be 6.1 K, and estimated values of 6.9 K and 6.3 K from the T_C trend in (a) were used for 3-ML and 4-ML film, respectively.

The data collapse of Fig. 3(b) can be understood within BCS theory in the following way. Starting with the mean-field gap equation *at zero temperature*,

$$\frac{1}{V} = \sum_{n}^{\varepsilon_n = E_D} \frac{1}{\sqrt{\Delta^2 + \varepsilon_n^2}}, \tag{2}$$

where V is the electron-phonon coupling as before, ε_n are the discrete single-particle energy levels on the island, and E_D is the Debye (phonon) energy as before, we can determine the dependence of Δ on the size of the island, which sets the spacing between the energy levels, ε_n. Since the lateral size of the islands is finite, one should in general use the gap equation with a discrete sum Eq. (2) rather than an integral Eq. (1). However, if the islands are large enough and one is looking at finite temperatures, the integral form Eq. (1) is a good approximation. That is the reason we have used it to fit our data earlier to obtain $\Delta(T)$. Here we wish to understand the fundamental reason that the suppression of superconductivity with lateral size follows a universal curve. For that purpose we begin with zero temperature considerations and then generalize to finite temperature to obtain the universal curve theoretically [see the black curve in Fig. 3(b)]. To understand weakened superconductivity in small islands, one must retain the discrete nature of the energy levels as their increased spacing with shrinking lateral size plays an important role in the suppression of superconductivity.[7,8,26] We first note that our data show an absence of Coulomb blockade effects on the islands, which would have a charging scale of $E_C \sim e^2/C$, which can be estimated as $E_C \sim$ 10–40 meV. Here e is the charge of the electron and the island capacitance $C = 2\pi\kappa L$, where L is the size of the dot and κ is the dielectric constant. This indicates some electrical contact with the substrate (also needed for the STM measurement itself), though we are not able to determine if the coupling is in the intermediate or strong regime. Because the contact of the SIC is only a "ring" around the Pb island (i.e., the Pb island is not "sitting" on the SIC), even a highly conducting SIC-Pb interface would only weakly affect the basic superconducting properties, which are primarily determined by the "bulk" island DOS and electron-phonon coupling. Thus, the essential physics of the universal suppression in our experiments is contained in Eq. (2), as we now show.

The typical scale of the variation in the DOS (number of energy levels on the island per unit energy) in Eq. (2) is set by the energy scale of the electronic degrees of freedom E_F (Fermi energy), which is 9.5 eV for Pb. On the other hand E_D is typically tens or hundreds of Kelvin (88 K in Pb), or roughly 10^{-2} electron volts. Because $E_D \ll E_F$, the DOS (i.e., average level spacing) will be constant to a good approximation over the energy range of the sum in Eq. (2), even for islands that are somewhat irregularly shaped. First consider an island with a shape that supports perfectly even space levels. (We will later show that when the energy levels are not perfectly spaced, there is very little change in the physics expressed through a self-consistency condition in the BCS-gap Eq. (2)—this is ultimately what is responsible for the universal suppression of the superconductivity.) When fluctuations in level separations are neglected $\varepsilon_n = n\delta$, where δ is the level spacing. The corresponding DOS for such an island is thus $1/\delta$.

From the well-known formula for the bulk gap in the thermodynamic limit, $\Delta_0 = 2E_D \exp\{-1/\lambda\} = 2E_D \exp\{-\delta/V\}$, and the bulk value of the transition temperature $T_C = \Delta_0/2.2 = 7.2$ K, we find $\delta/V = 2.5$ for Pb under the equal-level spacing assumption $\varepsilon_n = \delta n$. Here V is the strength of the electron-phonon coupling in units of energy. Thus, for the critical island size where the gap $\Delta = 0$, we have

$$2.5 = \frac{\delta}{V} = \sum_{n=1}^{n_{\max,0} = E_D/\delta} \frac{1}{n}, \tag{3}$$

which implies that $n_{\max,0} = 7$ when the island becomes so small that the transition temperature vanishes, or that $\delta = E_D/7 \sim 13$ K is roughly of the order of the bulk gap $\Delta_0 = 12$ K. The key analytical feature of Eq. (3) is the "$1/n$" contribution from the different energy levels: Even for large n, there are appreciable contributions to the sum ($1/n$ is logarithmically divergent). This means that any random (not too large) fluctuations from the equal-level spacing approximation attributable to an irregular-shaped island will be approximately averaged out. (We have verified this in numerical checks with random energy spacings constrained to have the same average.) Moreover, in islands larger than the critical size (with smaller level spacing δ) there will be *even more effective averaging* because the larger "small" n contributions will carry less weight because

of the presence of the gap in the denominator of Eqs. (2) and (4), and there will be more terms in the sum to be averaged, $n_{\max} > n_{\max,0}$:

$$2.5 = \frac{\delta}{V} = \sum_{n=1}^{n_{\max}=E_D/\delta} \frac{1}{\sqrt{\left(\frac{\Delta}{\delta}\right)^2 + n^2}}. \quad (4)$$

From Eq. (4) the gap dependence on level spacing $\Delta(\delta)$ is determined. We emphasize this analysis is valid even in the presence of tunneling coupling of the island states to the substrate, with only a small numerical change in the results. The previous arguments are not simply hand waving but rather rely on the properties of the summation of $1/n$ for a finite number of terms.

As we now show, similar considerations apply to the level-spacing dependence of the *critical temperature*, T_C, which is proportional to the gap. Formally, the temperature dependence of the gap in a small island is given by the discrete version of Eq. (1),

$$2.5 = \frac{\delta}{V} = \sum_{n=1}^{n_{\max}=E_D/\delta} \frac{\mathrm{Tanh}[\sqrt{(\Delta(T))^2 + (n\delta)^2}/(2k_BT)]}{\sqrt{\left(\frac{\Delta(T)}{\delta}\right)^2 + n^2}}, \quad (5)$$

which will exhibit the same insensitivity to level-spacing fluctuation as Eq. (4). The critical temperature T_C is given by Eq. (5) with $\Delta(T_C) = 0$,

$$2.5 = \frac{\delta}{V} = \sum_{n=1}^{n_{\max}=E_D/\delta} \frac{\mathrm{Tanh}[n\delta/(2k_BT_C)]}{n}. \quad (6)$$

For islands of equal volume but different shape the value of $n_{\max}$ in Eq. (6) will be roughly the same, since that only counts the total number of states in the energy window within E_D of the Fermi energy, and that number is expected to be a weak function of island shape [distorting a regularly shaped island into an irregular shape mainly rearranges energy levels, which is unimportant because of the "averaging" effect from the slow decay of the summand in Eq. (5)]. We believe the effective averaging of level-spacing fluctuations attributable to a roughly constant *average* DOS over the relevant energy range E_D is the reason we find that the normalized critical temperature curves in Fig. 3(b) collapse to a universal form that is to a good approximation independent of island shape and given by Eq. (6). We remark that first principles calculations have predicted some changes in the phonon spectrum and electron-phonon coupling, but this makes a quantitatively small change in the transition temperature in the thin-film geometry.[19] We believe our argument based on the BCS mean-field gap equation simply explains all the trends in our data and related experiments.[5,9]

In summary we have performed a STM/STS study of 2-d superconducting islands with different thicknesses and lateral sizes. As the lateral dimension is reduced, the strength of the superconducting order parameter is also reduced, first slowly at a dimension larger than the bulk coherence length, then dramatically at a critical length scale of 40 $\sim$ 50 nm, which corresponds to level spacing of order the bulk gap Δ. Interestingly the systematic suppression of superconductivity with size depends to a good approximation only on the volume of the island and is independent of its shape. We have explained this feature with theoretical arguments based on BCS theory. We expect this work to have broad implications for device implementation that depends on detailed knowledge of size-dependent superconductivity and to stimulate further fundamental studies on nanoscale superconductivity.

ACKNOWLEDGMENTS

This work was supported by NSF Grants No. DMR-0906025, CMMI-0928664, Welch Foundation F-1672, and Texas Advanced Research Program 003658-0037-2007. GAF acknowledges support by ARO W911NF-09-1-0527 and NSF DMR-0955778.

APPENDIX A: DETERMINATION OF THE SUPERCONDUCTING GAP

1. Normalization of tunneling spectra

Because of the existence of quantum-well states, the DOS of the sample is often not a constant within the relevant energy window of $E_F \pm 20$ meV. Consequently the raw dI/dV data contains an asymmetric background. Moreover, as will be discussed in Appendix B, there exist "pseudogap" features (the depression in dI/dV in the range between -10 mV to 10 mV) at temperature above T_C.[16] These two factors—the nonconstant DOS near E_F and the pseudogap—need to be considered in the normalization procedure. In most cases one can normalize the spectra by dividing them with the spectra acquired above T_C, which should represent the normal-state DOS. However, because of the existence of the pseudogap such a normalization procedure will artificially raise the dI/dV value in the vicinity of the superconducting gap, thus distorting the lineshape [see Figs. 4(a) and 4(b)]. We found that the spectra normalized in this manner would not fit well with a BCS-like gap function (discussed subsequently). Another possibility is to use spectra acquired at a temperature much above T_C (say, >80 K) to represent the normal-state DOS. However, the thermal drift encountered with such a large temperature change makes it difficult to guarantee that the tip will stay at the same location with respect to the sample.

Here we use a modified normalization procedure by using a high-order (in this case 5th-order) polynomial to fit the spectra

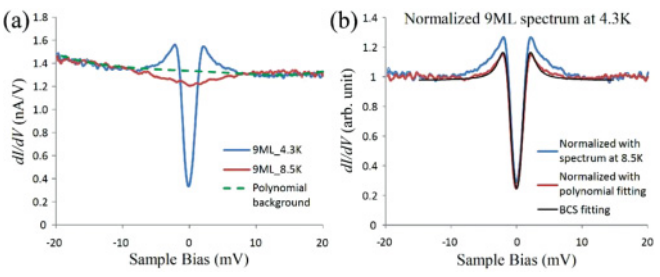

FIG. 4. (Color online) (a) dI/dV tunneling spectra obtained from 9-ML Pb films at 4.3 K and 8.5 K. (b) The result of normalization with the spectrum acquired at 8.5 K (blue line) and the 5th-order polynomial fitting (red line).

outside the gap region to represent the normal DOS [see the dashed line in Fig. 4(a)]. The resulting normalized spectra are shown in the red line of Fig. 4(b). This normalization procedure works quite well for a general shape even when the normal DOS contains a dip or peak. Moreover, it can be incorporated into a computer program that can automatically generate the normalized spectra without human bias. We recognize, however, the existence of pseudogap degrades the precision of fitting a small gap for spectra acquired very close to T_C. Consequently we regard those gap values below 0.2 meV as unreliable data and they are excluded from the T_C fitting.

2. Gap fitting

While the BCS-gap function[1] is not strictly applicable to the case of strong coupling like Pb, it remains a good approximation. Within this approximation, the differential conductance (dI/dV) based on the tunneling current between a normal metal (STM tip) and a superconductor (sample) can be expressed as

$$\frac{dI}{dV} \propto \int_{\Delta}^{\infty} \frac{|E|}{\sqrt{E^2-\Delta^2}} \left[-\frac{df}{dE}(E+eV)\right] dE, \quad \text{(A1)}$$

where $f(E)$ is the Fermi distribution function, V is an applied voltage bias, and Δ is the superconducting energy gap. In addition a Gaussian broadening of finite width (called the broadening parameter) is applied. This broadening is attributable to the incomplete shielding of the RF interference present at the tunneling junction, as we will subsequently discuss.

For each RF-shielding configuration there is only one broadening parameter. This parameter changes when the configuration of the RF shielding changes. Shown in Figs. 5(a) and 5(b) are results of STS measurement of 9 ML without the RF filter and with our best filter configuration we have achieved so far, respectively. For the no-filter configuration, a 0.8 meV broadening parameter is needed to fit the spectra,

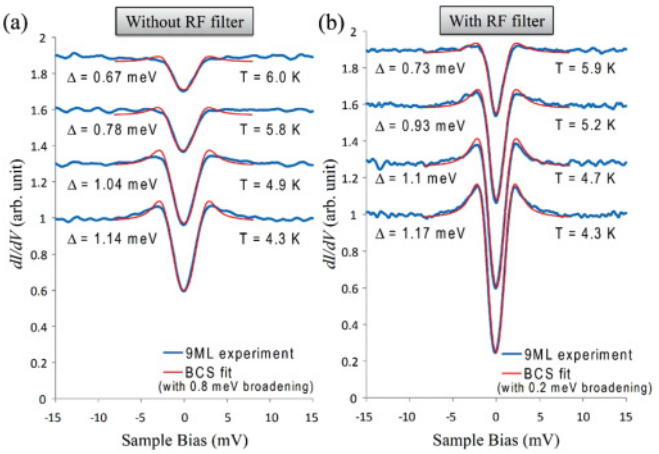

FIG. 5. (Color online) Temperature dependence of superconducting gap spectra taken from 9-ML Pb films (a) without RF filter and (b) with RF filter. 0.8-meV and 0.2-meV broadening were applied in the BCS DOS (red lines) of (a) and (b), respectively. Each normalized spectrum is offset successively by 0.3 for clarity.

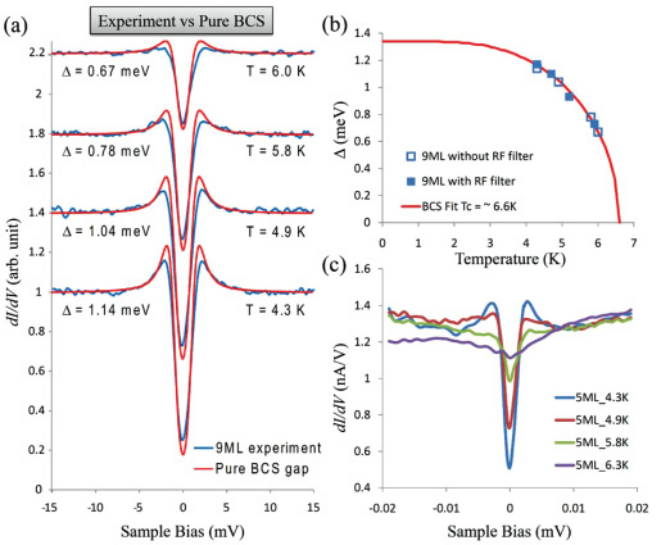

FIG. 6. (Color online) (a) Direct comparison between experimental spectra measured from 9-ML Pb films with our best RF shielding configuration and theoretical BCS DOS without any broadening. Each spectrum is offset successively by 0.4 for clarity. (b) The superconducting energy gaps (Δ) obtained from Figs. 5(a) and 5(b) were plotted as empty and solid blue squares for each temperature, respectively (error bar for each Δ value is smaller than the size of square mark). The red curve is a fitting of these energy gap data using a BCS gap equation. Those gap values from two shielding configurations align very well with a single BCS curve within a T_C of $\sim 6.6 \pm 0.1$ K. (c) Temperature dependent gap spectra measured from 5-ML Pb films.

corresponding to a RF noise with rms amplitude of 0.8 mV. On the other hand with a good RF-shielding configuration, only 0.2 meV broadening is needed. For a comparison we also show the theoretical spectra at different temperatures without any broadening in Fig. 6(a). One can see that the spectra acquired with our best RF-shielding configuration are reasonably close to the theoretical curves. It should be noted that in the temperature range where the spectra were acquired, the width of the Fermi-Dirac distribution already exceed the broadening parameter typically used in our experiments.

Most importantly while the raw data of the two configurations differ significantly in their line shape, they yield a very similar T_C (to within ± 0.1 K). In Fig. 6(b) we fit the gap values as a function of temperature from these two different configurations (shown as empty and solid squares). As one can see from this plot, the data from different filter configurations fall quite well onto a single BCS-like $\Delta(T)$ curve.

The best RF-shielding configuration used in the experiment unfortunately compromises the operation of the LT walker, which is an important component of LT-STM. Thus, for most of the experimental results reported in the main text, the spectra were acquired in a different RF-filter configuration, corresponding to a 0.3-meV broadening parameter. This second RF-filter configuration allows us to simultaneous operate the ultra-high-vacuum LT walker. Since we have shown that the fitted gap and the resulting T_C are independent of the

broadening parameter being used to within ±0.1 K, we believe the scientific conclusions would be consistent. We should also emphasize that the temperature dependence of the gap near T_C provides the most reliable determination of T_C because the gap varies most rapidly close to T_C. This can be clearly seen by observing the raw data of a 5-ML film in Fig. 6(c); while at 5.8 K, the superconducting gap is still clearly observable, it disappears at 6.3 K, consistent with the fitted T_C value of 6.1 K.

APPENDIX B: THE PSEUDOGAP STRUCTURE AT VOLTAGES ABOVE THE GAP

The majority of this paper is focused on the superconducting properties of nano-islands of different thicknesses and shapes. However, our data also show interesting features at voltage biases above the gap when the temperature is below T_C and for all voltages we probed when the temperature is above T_C. As seen in Figs. 7(a) and 7(b) (where the temperature is above T_C), there is a "pseudogap" feature that appears (even for very large islands). The pseudogap does not measurably change when the temperature drops below T_C, suggesting that it is likely an intrinsic property of the normal state of the Pb islands and not related to superconductivity in any way. It has been suggested in an earlier study[16] on films that such features may be attributable to phonon effects. We show here that we obtain a very good fit to a theory based on a pseudogap feature arising only from the combined influences of electron-electron interactions and disorder.[27] Moreover, we are able to extract a quantitative estimate of the *normal state* conductivity of the Pb nano-islands used in our experiments.

According to Ref. 26, the tunneling DOS should follow a form

$$\frac{dI}{dV} = c_1 + c_2 |V|^{\alpha} + mV, \tag{B1}$$

where c_1, c_2, α, and m all depend on details of the system, and V is the voltage. The final term mV accounts for a weakly energy-dependent tunneling-matrix element between the STM tip and the Pb substrate rather than intrinsic island properties and does not enter our estimates of island conductivity. For our purposes we are most interested in α as it is inversely proportional to the 2-d conductance of the nano-island/thin film substrate

$$\alpha = \frac{e^2}{h\sigma} \frac{\ln(2\pi a e^2 dn/d\mu)}{2\pi}, \tag{B2}$$

where e is the charge of the electron, h is Planck's constant, σ is the 2-d conductivity of the island or film, a is the tip-sample spacing, and $dn/d\mu$ is the compressibility of the island or film. (Here n is the 2-d density and μ the chemical potential.) Because the expression is only logarithmically dependent on the compressibility, we can estimate it by using a free-electron approximation. For 2-d electrons $dn/d\mu = 4\pi m^*/h^2$, where $m^* = 1.14\, m_e$ is the effective mass of Pb, and m_e is the bare mass of the electron.[28]

The plots of conductance vs island size are given in Figs. 7(c) and 7(d) for 3-ML- and 4-ML-film thicknesses. The values are consistent with those measured in early film samples,[29,30] *but here we provide the first conductance measurements of islands*. The general trend is for thicker and larger islands to be more conducting and for the conductance to be higher as the temperature is lowered. These findings are all consistent with expectations. Figure 8 shows that the pseudogap feature at energies above the gap does not change as the temperature drops below the superconducting transition temperature.

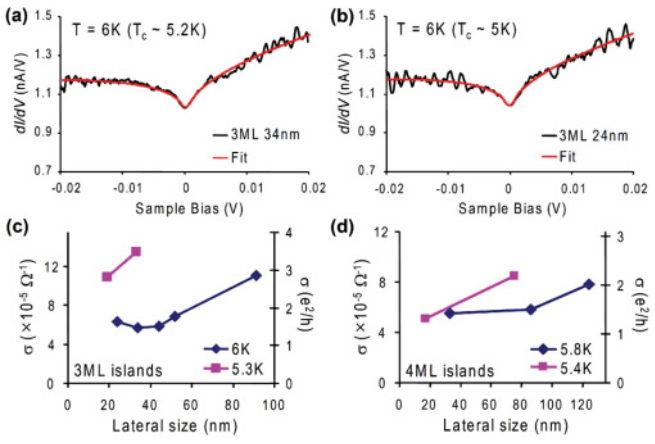

FIG. 7. (Color online) (a,b) Comparison of dI/dV spectrum measured at 6 K (above T_C) for 3-ML islands and theoretical tunneling DOS based on electron-electron interaction and disorder [Eq. (B1)]. Because $T = 0$ K is assumed in Eq. (B1), 1.2-meV broadening effect is applied to the fitting curves to take finite temperature and instrument noise into account. (c,d) 2-d conductivity (σ) values for Pb islands obtained from the fitting result in (a,b).

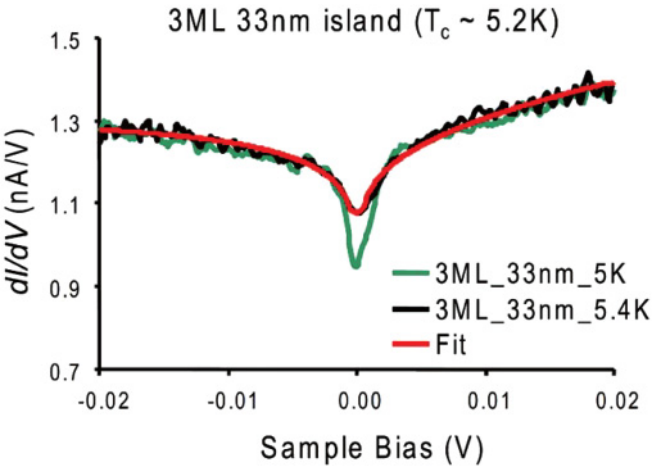

FIG. 8. (Color online) Shown is a comparison of the pseudogap feature at temperatures below and above the superconducting transition temperature. The lack of any clear temperature dependence for energies above the gap [clear from fit to Eq. (B1)] indicates the high-energy part of the pseudogap is not related to superconductivity but is rather a normal-state property of the Pb nano-islands.

*shih@physics.utexas.edu

[1] J. Bardeen, L. N. Cooper, and J. R. Schrieffer, Phys. Rev. **108**, 1175 (1957).

[2] D. C. Ralph, C. T. Black, and M. Tinkham, Phys. Rev. Lett. **74**, 3241 (1995).

[3] T. Zhang, P. Cheng, W. J. Li, Y. J. Sun, G. Wang, X. G. Zhu, K. He, L. L. Wang, X. C. Ma, X. Chen, Y. Y. Wang, Y. Liu, H. Q. Lin, J. F. Jia, and Q. K. Xue, Nat. Phys. **6**, 39 (2010).

[4] S. Y. Qin, J. Kim, Q. Niu, and C. K. Shih, Science **324**, 1314 (2009).

[5] S. Bose, A. M. Garcia-Garcia, M. M. Ugeda, J. D. Urbina, C. H. Michaelis, I. Brihuega, and K. Kern, Nat. Mater. **9**, 550 (2010).

[6] K. Clark, A. Hassanien, S. Khan, K. F. Braun, H. Tanaka, and S. W. Hla, Nat. Nanotechnol. **5**, 261 (2010).

[7] R. A. Smith and V. Ambegaokar, Phys. Rev. Lett. **77**, 4962 (1996).

[8] J. von Delft, A. D. Zaikin, D. S. Golubev, and W. Tichy, Phys. Rev. Lett. **77**, 3189 (1996).

[9] I. Brihuega, S. Bose, M. M. Ugeda, C. H. Michaelis, and K. Kern, e-print arXiv:0904.0354v1.

[10] M. M. Ozer, J. R. Thompson, and H. H. Weitering, Nat. Phys. **2**, 173 (2006).

[11] D. Eom, S. Qin, M. Y. Chou, and C. K. Shih, Phys. Rev. Lett. **96**, 027005 (2006).

[12] G. J. Dolan and J. Silcox, Phys. Rev. Lett. **30**, 603 (1973).

[13] R. C. Dynes, A. E. White, J. M. Graybeal, and J. P. Garno, Phys. Rev. Lett. **57**, 2195 (1986).

[14] Z. L. Guan, Y. X. Ning, C. L. Song, J. Wang, J. F. Jia, X. Chen, Q. K. Xue, and X. C. Ma, Phys. Rev. B **81**, 054516 (2010).

[15] C. Brun, I. P. Hong, F. Patthey, I. Y. Sklyadneva, R. Heid, P. M. Echenique, K. P. Bohnen, E. V. Chulkov, and W. D. Schneider, Phys. Rev. Lett. **102**, 207002 (2009).

[16] K. Wang, X. Zhang, M. M. T. Loy, T. C. Chiang, and X. Xiao, Phys. Rev. Lett. **102**, 076801 (2009).

[17] Y. Guo, Y. F. Zhang, X. Y. Bao, T. Z. Han, Z. Tang, L. X. Zhang, W. G. Zhu, E. G. Wang, Q. Niu, Z. Q. Qiu, J. F. Jia, Z. X. Zhao, and Q. K. Xue, Science **306**, 1915 (2004).

[18] I. Hetel, T. R. Lemberger, and M. Randeria, Nat. Phys. **3**, 700 (2007).

[19] J. Noffsinger and M. L. Cohen, Phys. Rev. B **81**, 214519 (2010).

[20] A. Yazdani and A. Kapitulnik, Phys. Rev. Lett. **74**, 3037 (1995).

[21] D. L. Miller, Phys. Rev. B **15**, 4180 (1977).

[22] M. Hupalo, T. L. Chan, C. Z. Wang, K. M. Ho, and M. C. Tringides, Phys. Rev. B **66**, 161410 (2002).

[23] E. Ganz, I. S. Hwang, F. L. Xiong, S. K. Theiss, and J. Golovchenko, Surf. Sci. **257**, 259 (1991).

[24] L. Seehofer, G. Falkenberg, D. Daboul, and R. L. Johnson, Phys. Rev. B **51**, 13503 (1995).

[25] M. Tinkham, *Introduction to Superconductivity* (Dover Publications, Mineola, New York, 1996), pp. 62–63.

[26] P. W. Anderson, J. Phys. Chem. Solids **11**, 26 (1959).

[27] L. S. Levitov and A. V. Shytov, e-print arXiv:cond-mat/9607136v1.

[28] B. J. Hinch, C. Koziol, J. P. Toennies, and G. Zhang, Europhys. Lett. **10**, 341 (1989).

[29] O. Pfennigstorf, K. Lang, H. L. Gunter, and M. Henzler, Appl. Surf. Sci. **162**, 537 (2000).

[30] O. Pfennigstorf, A. Petkova, Z. Kallassy, and M. Henzler, Eur. Phys. J. B **30**, 111 (2002).